

# UC Irvine

## UC Irvine Previously Published Works

### Title

Ground-level ozone in four Chinese cities: precursors, regional transport and heterogeneous processes

### Permalink

<https://escholarship.org/uc/item/6s9805qh>

### Journal

Atmospheric Chemistry and Physics, 14(23)

### ISSN

1680-7316

### Authors

Xue, LK  
Wang, T  
Gao, J  
[et al.](#)

### Publication Date

2014

### DOI

10.5194/acp-14-13175-2014

### Copyright Information

This work is made available under the terms of a Creative Commons Attribution License, available at <https://creativecommons.org/licenses/by/4.0/>

Peer reviewed



# Ground-level ozone in four Chinese cities: precursors, regional transport and heterogeneous processes

L. K. Xue<sup>1,2</sup>, T. Wang<sup>1,2,3</sup>, J. Gao<sup>3</sup>, A. J. Ding<sup>4</sup>, X. H. Zhou<sup>2</sup>, D. R. Blake<sup>5</sup>, X. F. Wang<sup>2</sup>, S. M. Saunders<sup>6</sup>, S. J. Fan<sup>7</sup>, H. C. Zuo<sup>8</sup>, Q. Z. Zhang<sup>2</sup>, and W. X. Wang<sup>2,3</sup>

<sup>1</sup>Department of Civil and Environmental Engineering, Hong Kong Polytechnic University, Hong Kong, China

<sup>2</sup>Environment Research Institute, Shandong University, Ji'nan, Shandong, China

<sup>3</sup>Chinese Research Academy of Environmental Sciences, Beijing, China

<sup>4</sup>Institute for Climate and Global Change Research and School of Atmospheric Sciences, Nanjing University, Nanjing, Jiangsu, China

<sup>5</sup>Department of Chemistry, University of California at Irvine, Irvine, CA, USA

<sup>6</sup>School of Chemistry and Biochemistry, University of Western Australia, Crawley, Perth WA, Australia

<sup>7</sup>College of Environmental Science and Engineering, Sun Yat-Sen University, Guangzhou, Guangdong, China

<sup>8</sup>College of Atmospheric Sciences, Lanzhou University, Lanzhou, Gansu, China

Correspondence to: L. K. Xue (xuelikun@gmail.com) and T. Wang (cetwang@polyu.edu.hk)

Received: 13 July 2014 – Published in Atmos. Chem. Phys. Discuss.: 12 August 2014

Revised: 12 October 2014 – Accepted: 18 October 2014 – Published: 10 December 2014

**Abstract.** We analyzed the measurements of ozone ( $O_3$ ) and its precursors made at rural/suburban sites downwind of four large Chinese cities – Beijing, Shanghai, Guangzhou and Lanzhou, to elucidate their pollution characteristics, regional transport, in situ production, and impacts of heterogeneous processes. The same measurement techniques and observation-based model were used to minimize uncertainties in comparison of the results due to difference in methodologies. All four cities suffered from serious  $O_3$  pollution but showed different precursor distributions. The model-calculated in situ  $O_3$  production rates were compared with the observed change rates to infer the relative contributions of on-site photochemistry and transport. At the rural site downwind of Beijing, export of the well-processed urban plumes contributed to the extremely high  $O_3$  levels (up to an hourly value of 286 ppbv), while the  $O_3$  pollution observed at suburban sites of Shanghai, Guangzhou and Lanzhou was dominated by intense in situ production. The  $O_3$  production was in a volatile organic compound (VOC)-limited regime in both Shanghai and Guangzhou, and a  $NO_x$ -limited regime in Lanzhou. The key VOC precursors are aromatics and alkenes in Shanghai, and aromatics in Guangzhou. The potential impacts on  $O_3$  production of several heterogeneous processes, namely, hydrolysis of dinitrogen pentoxide ( $N_2O_5$ ), uptake

of hydro peroxy radical ( $HO_2$ ) on particles and surface reactions of  $NO_2$  forming nitrous acid (HONO), were assessed. The analyses indicate the varying and considerable impacts of these processes in different areas of China depending on the atmospheric abundances of aerosol and  $NO_x$ , and suggest the urgent need to better understand these processes and represent them in photochemical models.

## 1 Introduction

Air quality in the metropolitan areas has drawn increasing attention in recent years (Molina and Molina, 2004; Parrish and Zhu, 2009). A typical and difficult issue is photochemical smog characterized by unhealthily high concentrations of ground-level ozone ( $O_3$ ), which is a product of atmospheric photochemistry involving nitrogen oxides ( $NO_x = NO + NO_2$ ) and volatile organic compounds (VOCs). The ozone problem is a complex coupling of primary emissions, chemical transformation, and dynamic transport at different scales (Jacob, 1999). Challenges in regulating  $O_3$  pollution primarily lie in understanding its non-linear chemistry with respect to precursors (i.e.,  $NO_x$ , CO

and VOCs) and contributions from both local and regional sources.

China has become home to several megacities and many large cities owing to its fast-paced urban-industrialization processes. It is not surprising that these cities have been experiencing air quality deterioration in light of their fast expansion in economics, energy use and motor vehicles in the past decades. High O<sub>3</sub> concentrations exceeding the national ambient air quality standards have been observed frequently in and downwind of large cities (e.g., Wang et al., 2006, 2010a; Zhang et al., 2007; Zhang et al., 2008; Ran et al., 2009; Chou et al., 2011). Recent studies also indicated increasing O<sub>3</sub> trends in several highly urbanized regions, i.e., the North China Plain (NCP; 1995–2005, Ding et al., 2008; 2005–2011, Zhang et al., 2014), Yangtze River delta (YRD; 1991–2006, Xu et al., 2008) and Pearl River delta (PRD; 1994–2007, Wang et al., 2009). Furthermore, a worsening prospect of the problem is even foreseen in view of the projected continuing increase in emissions of NO<sub>x</sub> and VOCs in the near future (Ohara et al., 2007). Consequently, effective control strategies based on scientifically sound knowledge must be in place in order to return to the clearer and cleaner skies.

Atmospheric models are the common tools used to understand the O<sub>3</sub> formation processes. The chemical mechanisms underlying the models are usually simplified representations of the complex atmospheric chemistry, with the organic species of similar reactivities and structures grouped into one model species (Stockwell et al., 2012). This chemical lumping gives reduced computational run times, but may produce extra uncertainties when applied to different atmospheric conditions (e.g., with different VOC emissions; the lumped mechanisms are usually optimized with emission estimates in some developed regions). The Master Chemical Mechanism (MCM) is a nearly explicit mechanism that has the minimum amount of chemical lumping (Jenkin et al., 2003; Saunders et al., 2003), and hence is the best choice to investigate atmospheric photochemistry for a variety of environments. Another source of uncertainty is heterogeneous chemical processes which have recently been found to be more complex than previously thought. Several cases in point are the hydrolysis of dinitrogen pentoxide (N<sub>2</sub>O<sub>5</sub>), uptake of hydro peroxy radical (HO<sub>2</sub>) on particles, and surface reactions of NO<sub>2</sub> forming nitrous acid (HONO) (Brown et al., 2006; Thornton et al., 2008; Su et al., 2011). These processes are believed to be more relevant in China given its very high aerosol loadings. However, they are usually neglected by most of the current mechanisms (such as MCM), and to date only very limited studies have attempted to evaluate their potential impacts and suggested the important role of HO<sub>2</sub> uptake in O<sub>3</sub> formation (e.g., Kanaya et al., 2009; Liu et al., 2012).

Another challenge in understanding ground-level O<sub>3</sub> problem is to dissect the local and regional contributions. Two types of methods have been widely used for this. One is the

chemical transport model that is ideal to quantify local and regional contributions but may be subject to uncertainties from the emission inventory estimates (Wang et al., 2010b; Tie et al., 2013). The other approach is observation-based and usually comprises concurrent measurements from at least a pair of stations (Wang et al., 2010a; Berlin et al., 2013). It assumes that the O<sub>3</sub> concentrations at the upwind site can be regarded as the regional background for the receptor site. To our knowledge, there are very limited studies that estimated the contributions of local production and regional transport based on the observations at a single locale (e.g., Frost et al., 1998).

To evaluate the atmospheric impacts of emerging Chinese megacities, intensive observations of O<sub>3</sub> and O<sub>3</sub> precursors were conducted from 2004 to 2006 in suburban/rural areas near four Chinese major cities, namely Beijing, Shanghai, Guangzhou, and Lanzhou. These cities are located in different regions of China (see Fig. 1) and have different geographies, climates, industries and emission patterns. The same measurement techniques were utilized in all campaigns to minimize uncertainties arising from experiments in comparison of the results. These studies generated much high-quality data in the mid-2000s in major urban areas of China, which will be invaluable for assessing the atmospheric impact of on-going rapid urbanization in China. For data analysis, an observation-based MCM model (OBM) was deployed to quantify the contributions of in situ photochemistry and regional transport and to assess the potential impacts of several heterogeneous processes. Overall, this study reveals the similarly serious O<sub>3</sub> pollution, different distributions in O<sub>3</sub> precursors, and varying impacts of heterogeneous chemistry in major cities of China.

## 2 Methodology

### 2.1 Study areas and sites

The field experiments were conducted in rural/suburban areas near three megacities in Northern (Beijing), Eastern (Shanghai) and Southern (Guangzhou) China, and a large city in Western China (Lanzhou; see Fig. 1). The sampling sites were selected carefully downwind of city centers during the study periods to allow investigation of regional-scale pollution and processes. These sites have been described separately by Wang et al. (2006); Gao et al. (2009); J. M. Zhang et al. (2009) and Pathak et al. (2009), and here we only give a brief outline.

Beijing is the capital city of China and among the largest cities in the world. It is located on the northwestern periphery of the densely populated North China Plain, and accommodates more than 19 million inhabitants, 5 million automobiles, and dozens of factories and power plants. The observations were carried out from 21 June to 31 July 2005 in a rural mountainous area in Chang Ping district (CP; 40°21'N,

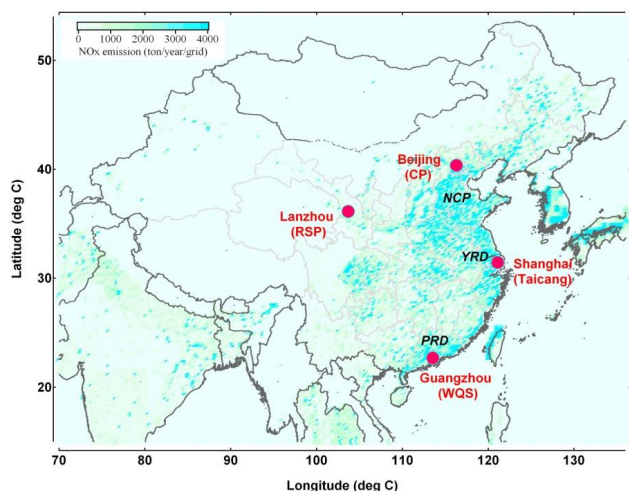


**Figure 1.** Map showing the study areas and anthropogenic  $\text{NO}_x$  emissions over China. The emission data were obtained from Q. Zhang et al. (2009).

116°18'E; 280 m a.s.l.), about 50 km north (generally downwind in summer) of the downtown. The site was in a fruit farm with sparse population and anthropogenic emissions about 10 km away (Wang et al., 2006). The rural nature of the site determines to a large extent the “unique” results obtained in Beijing (i.e., highest  $\text{O}_3$ , lowest  $\text{O}_3$  precursors, and dominant role of regional transport) compared to the other three cities (suburban sites), which should be kept in mind when comparing the results among the four sites.

Shanghai is the largest city of China and located in the Yangtze River Delta. It has over 23 million population, 2 million vehicles, China's largest petrochemical complex, steel manufacturer, seaport and other industries. The study site was in the Taicang Meteorological Station (31°27'N, 121°06'E; 20 m a.g.l.), which is approximately 45 km northwest of Shanghai. Although Taicang belongs to Jiangsu Province, it is often affected by urban plumes of Shanghai under the prevailing southeasterly winds in the summer-monsoon season. The observations taken from 4 May to 1 June 2005 were analyzed in the present study.

Guangzhou is a megacity of over 12 million people in southern China. It is in the center of the Pearl River Delta, which has been a “world factory” for a wide range of consumer products. The measurements were made at Wan Qing Sha (WQS; 22°42'N, 113°33'E; 17 m a.g.l.), a suburban area about 50 km southeast of downtown Guangzhou. The data collected between 20 April and 26 May 2004 were analyzed in this paper. Thus the present study targets the  $\text{O}_3$  pollution in late spring, and can be compared with and supplement previous investigations that focused on autumn (Zhang et al., 2007; Zhang et al., 2008).

Lanzhou is a large city of over 3 million people and an industrial center in the interior western China. It is situated in a narrow valley basin in a mountainous region with a mean al-

titude of 1520 m a.s.l. This unique topography, together with its petrochemical industry as well as vehicle emissions (0.2 million cars in 2006), makes it a typical “basin” of  $\text{O}_3$  pollution in summer (Zhang et al., 2000). The sampling site was located in Renshoushan Park (RSP; 36°8'N, 103°41'E), a suburban mountainous area with some peach trees and other vegetation (J. M. Zhang et al., 2009). The industrial zone (Xigu petrochemical district) is located about 5 km to the southwest, and the urban center is about 15 km to the southeast. The intensive campaign was conducted from 19 June to 16 July 2006.

## 2.2 Measurement techniques

The same set of techniques were deployed to measure  $\text{O}_3$ ,  $\text{CO}$ ,  $\text{SO}_2$ ,  $\text{NO}$ ,  $\text{NO}_y$ , VOCs, particle number and size distribution, and meteorological parameters at the four cities.  $\text{O}_3$  was monitored by a UV photometric instrument (*Thermo Environmental Instruments (TEI), Model 49i*).  $\text{CO}$  was measured by a non-dispersive infrared analyzer (*Advanced Pollution Instrumentation, Model 300EU*) with internal zeroing automatically done every 2 h.  $\text{SO}_2$  was observed with a pulsed UV fluorescence analyzer (*TEI Model 43c*).  $\text{NO}$  and  $\text{NO}_y$  were detected by a chemiluminescence analyzer (*TEI Model 42cy*) coupled with an external molybdenum oxide catalytic converter to reduce  $\text{NO}_y$  to  $\text{NO}$  (Xue et al., 2011). Aerosol number and size distribution (10 nm–10  $\mu\text{m}$ ) were measured in real-time under ambient humidity conditions by a wide-range particle spectrometer (*MSP, WPS model 1000XP*) in Beijing, Shanghai and Lanzhou. Temperature, pressure, relative humidity (RH), wind direction and speed, and solar radiation were continuously measured by a weather station. All the above measurement techniques and quality assurance/control procedures have been described elsewhere (Gao et al., 2009; Xue et al., 2011).

Methane and  $\text{C}_2$ – $\text{C}_{10}$  non-methane hydrocarbons (NMHCs) were measured by collecting whole air samples in evacuated stainless-steel canisters with subsequent analysis by gas chromatography with flame ionization detection, electron capture detection, and mass spectrometry (the analysis was undertaken in the University of California at Irvine) (Xue et al., 2013). Generally, one sample was collected at noon each day during the field campaigns (note that the sampling was not made consecutively at Lanzhou). In addition, multiple samples were taken on selected ozone episode days, normally one sample every 2 h from 07:00 to 19:00 LT. Such a sampling strategy aimed at facilitating both a thorough evaluation of VOC pollution for the campaigns and a comprehensive modeling analysis for the high  $\text{O}_3$  events. In total, 130, 68, 76, and 24 VOC samples were collected in Beijing, Shanghai, Guangzhou, and Lanzhou, respectively.

### 2.3 Observation-based model

An observation-based chemical box model was utilized to quantify the in situ O<sub>3</sub> production. The model has been successfully applied in the previous studies (Xue et al., 2013, 2014a, b). Briefly, it is built on the Master Chemical Mechanism (v3.2), a nearly explicit mechanism describing oxidation of 143 primary VOCs together with the latest IUPAC inorganic nomenclature (Jenkin et al., 2003; Saunders et al., 2003). In addition, heterogeneous processes including uptake of N<sub>2</sub>O<sub>5</sub>, NO<sub>3</sub> and HO<sub>2</sub> on aerosols and reactions of NO<sub>2</sub> on ground/particle surfaces producing HONO are also incorporated (see details in Sect. 3.3). Dry depositions of inorganic gases, peroxides, PANs, carbonyls and organic acids are adopted in the model from the recent compilation (Zhang et al., 2003). The mixing-layer height affecting dry deposition rates was assumed to vary from 300 m at night to 1500 m in the afternoon. Sensitivity model runs with other maximum mixing heights (i.e., 1000 and 2000 m) showed that its impact on the modeling results was negligible (i.e., < 3% in net O<sub>3</sub> production rates).

The observed data of O<sub>3</sub>, CO, SO<sub>2</sub>, NO, CH<sub>4</sub>, C<sub>2</sub>–C<sub>10</sub> NMHCs, H<sub>2</sub>O, temperature, pressure, and aerosol surface and radius were averaged or interpolated with a time resolution of 1 h and used as the model inputs. The aerosol surface and radius were calculated from the aerosol number and size distribution measurements. For Guangzhou where such measurements were not available, we used the average diurnal data obtained from a similar suburban site in Hong Kong (Tung Chung, close to the WQS site; see Fig. S1 in the Supplement) in the same season (May 2012). Sensitivity studies using 50% higher aerosol surface indicated little impact on the modeling results (i.e., ~ 1% in net O<sub>3</sub> production rate). For hydrocarbons for which the observations were not in real-time, the time-dependent concentrations at hourly resolution were estimated as follows. During the daytime (i.e., 07:00–19:00 LT) when multiple samples were taken, the data gaps were filled by time interpolation. The nighttime concentrations were estimated based on the regressions with CO (for most hydrocarbons except for isoprene) and temperature (for isoprene), for which continuous measurements were available. Photolysis frequencies were computed as a function of solar zenith angle (Saunders et al., 2003), and were further scaled by the measured solar radiation. The model calculations were made for the identified O<sub>3</sub> episode days with 00:00 LT as the initial time. Before each simulation, the model pre-ran for 9 days with constraints of the campaign-average data so that the model approached a steady state for the unmeasured species (e.g., NO<sub>2</sub> and radicals).

The model read the inputs every hour to calculate the in situ O<sub>3</sub> production and destruction rates. The ozone production rates calculated by the OBM usually correspond to the production of total oxidant (O<sub>x</sub> = O<sub>3</sub> + NO<sub>2</sub>) other than O<sub>3</sub> alone (by considering the oxidation of NO to NO<sub>2</sub> by peroxy radicals; Kanaya et al., 2009; Xue et al., 2013). Here we de-

termined directly the reaction rates of O<sub>3</sub> instead of O<sub>x</sub> with our model. In the troposphere, O<sub>3</sub> production is eventually achieved by the combination of an O atom with O<sub>2</sub> (Reaction R1), and O<sub>3</sub> destruction is mainly facilitated by O<sub>3</sub> photolysis (Reaction R2) and reactions with NO (Reaction R3), NO<sub>2</sub> (Reaction R4), OH (Reaction R5), HO<sub>2</sub> (Reaction R6), atoms of O (Reaction R7) and Cl (Reaction R8), and unsaturated VOCs (Reaction R9) (In general, the O<sub>3</sub> destruction was dominated by reactions of (R2)–(R4), while the other reactions may also make considerable contributions at specific conditions (e.g., at high VOCs).



Thus the O<sub>3</sub> production and destruction rates can be calculated as

$$P(\text{O}_3) = k_1 [\text{O}_2][\text{O}][M] \quad (1)$$

(*M* denotes N<sub>2</sub> or O<sub>2</sub>)

$$L(\text{O}_3) = J_{\text{O}_3}[\text{O}_3] + k_3[\text{NO}][\text{O}_3] + k_4[\text{NO}_2][\text{O}_3] + k_5[\text{OH}][\text{O}_3] + k_6[\text{HO}_2][\text{O}_3] + k_7[\text{O}][\text{O}_3] + k_8[\text{Cl}][\text{O}_3] + \sum (k_{9i}[\text{VOC}_i])[\text{O}_3] \quad (2)$$

Then the net O<sub>3</sub> production rate can be determined from the difference between *P*(O<sub>3</sub>) and *L*(O<sub>3</sub>). We also compared our-derived O<sub>3</sub> net rates with those of O<sub>x</sub> from the traditional method, and found both methods showed overall good agreement (see Fig. S2).

### 3 Results and discussion

#### 3.1 Overview of O<sub>3</sub> and O<sub>3</sub> precursors

Table 1 summarizes the overall O<sub>3</sub> pollution conditions observed in the four cities. At the rural site of Beijing, 18 O<sub>3</sub> episode days (here defined as days when the peak hourly O<sub>3</sub> exceeded 100 ppbv; 44 % of the total) were observed during the 6-week measurement period. The maximum hourly O<sub>3</sub> mixing ratio was 286 ppbv, which is by far the highest value reported in China in open literatures (Wang et al., 2006). Such frequency of episodes and extreme O<sub>3</sub> levels highlight the serious problem in the Beijing area. At the suburban site near Shanghai, 6 episode days (21 %) occurred during the 4-week campaign with the maximum hourly O<sub>3</sub> of 127 ppbv observed. The pollution in Shanghai (YRD) seemed relatively lighter than those in other three cities, which may be due to the titration effect of its high NO<sub>x</sub> levels (Ding et al., 2013). At the downwind site of Guangzhou, seven episodes (19 %) were encountered throughout the 37 measurement days. The maximum hourly O<sub>3</sub> concentration was recorded at 178 ppbv. This indicates that the O<sub>3</sub> pollution in the PRD is serious not only in autumn but also in late spring. In Lanzhou, eight episodes (29 %) took place during the 4-week campaign with a maximum hourly O<sub>3</sub> of 143 ppbv. Our observations highlight the serious ozone pollution in the large cities of China.

We then examined the distributions of major O<sub>3</sub> precursors observed in the four cities. The mean diurnal profiles of NO<sub>y</sub> and CO are shown in Fig. 2. At the rural site of Beijing with few local emissions, both precursors showed high levels in the late afternoon till the evening, corresponding to regional transport of urban plumes. At the suburban sites downwind of Shanghai, Guangzhou and Lanzhou, in comparison, they exhibited a morning maximum and/or another evening peak, which were mainly caused by the shallow boundary layer and enhanced emissions in the rush hours. The NO<sub>y</sub> levels measured in Shanghai (24–39 ppbv) and Guangzhou (24–52 ppbv) were significantly higher than those in Beijing (rural site; 11–16 ppbv) and Lanzhou (7–27 ppbv), while the CO levels were comparable in the four cities despite the relatively lower afternoon concentrations in Lanzhou.

Figure 3 documents the average reactivities towards OH of major hydrocarbons in the four cities (see Supplement for the OH reactivity calculation). To facilitate interpretation of the hydrocarbon speciation, the 50+ species were categorized into anthropogenic hydrocarbons (AHC; encompassing most species except for isoprene and  $\alpha/\beta$ -pinenes) and biogenic hydrocarbons (BHC; comprising isoprene and  $\alpha/\beta$ -pinenes), with AHC further grouped into reactive aromatics (R-AROM; including all aromatics except for benzene), alkenes, alkanes with  $\geq 4$  carbons (C4HC), and low-reactivity hydrocarbons (LRHC; including methane, ethane, propane, acetylene and benzene; see Table S1 in the Supplement). The highest hydrocarbon reactivity was determined

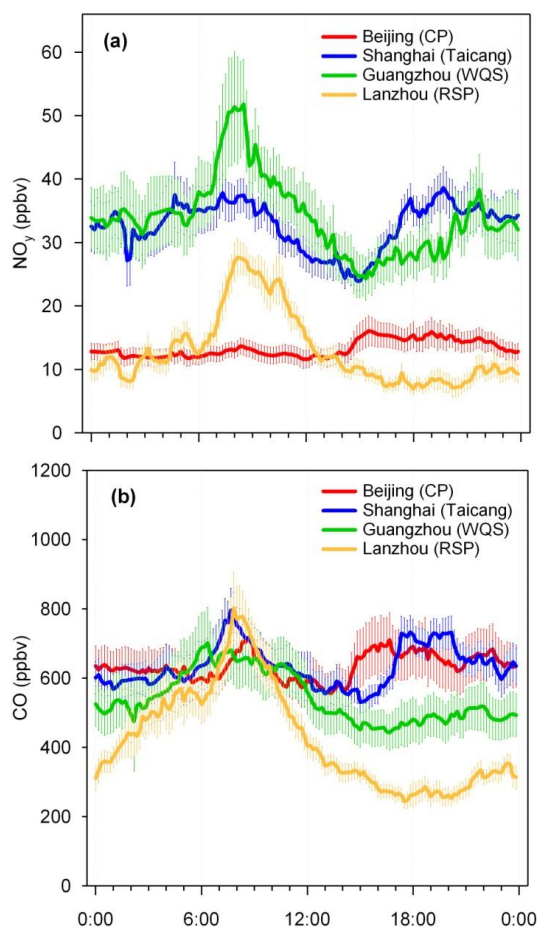


**Figure 2.** Observed average diurnal profiles of (a) NO<sub>y</sub> and (b) CO in the four cities. The data time interval is 10 min, and the error bar is standard error.

in Lanzhou ( $9.33 \text{ s}^{-1}$  in total), followed by those in Shanghai ( $5.85 \text{ s}^{-1}$ ) and Guangzhou ( $5.23 \text{ s}^{-1}$ ). This is opposite to the patterns for NO<sub>y</sub> and CO as shown in Fig. 2. The lowest reactivity ( $2.77 \text{ s}^{-1}$ ) was measured at the Beijing site, which should be ascribed to the fact that our site is located in a rural mountainous area with few local anthropogenic emissions. It also implies that the urban plumes had undergone extensive photochemical processing during transport and were less reactive when reaching the Beijing site.

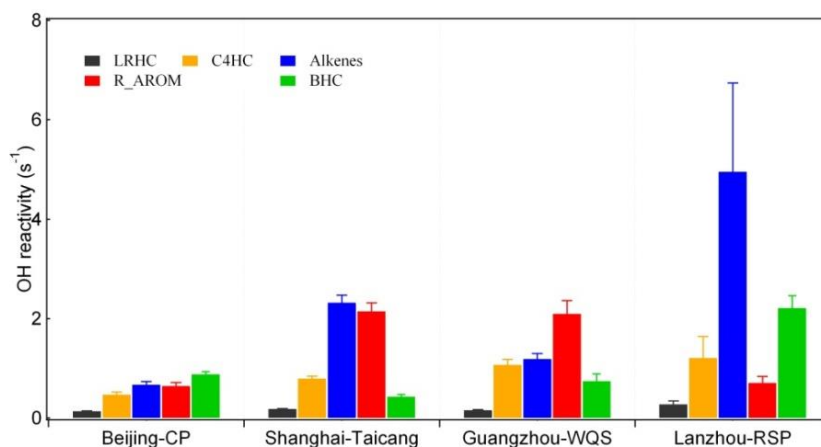
Furthermore, different hydrocarbon distributions among the four cities were also illustrated. In Beijing and Shanghai, the AHC reactivities were dominated by both alkenes (35 and 43 %) and R-AROM (34 and 39 %). In Guangzhou, R-AROM was the dominant AHC class with an average contribution of 46 %. And in Lanzhou, alkenes played a predominant role and composed on average 70 % of the AHC reactivity. In particular, the propene and ethene levels were extremely high, both of which contributed 53 % of the AHC reactivity. These results suggest distinct emission patterns of



**Table 1.** Overview of ozone pollution conditions in four Chinese cities.

Site	Location	Observation period	Number of O <sub>3</sub> episode days*	Maximum hourly O <sub>3</sub> (ppbv)
Beijing CP	116.30° E, 40.35° N	June 21–July 31 2005	18	286
Shanghai Taicang	121.10° E, 31.45° N	May 4–June 1 2005	6	127
Guangzhou WQS	113.55° E, 22.70° N	April 20–May 26 2004	7	178
Lanzhou RSP	103.69° E, 36.13° N	June 19–July 16 2006	8	143

\* The ozone episode day is defined here as the one with the maximum hourly ozone exceeding 100 ppbv.

**Figure 3.** Average OH reactivities of major hydrocarbons at the four cities. The error bar is standard error.

O<sub>3</sub> precursors and imply different O<sub>3</sub> formation regimes in the four cities (see next section).

### 3.2 Process analysis: regional transport vs. in situ formation

To understand the processes contributing to high O<sub>3</sub> pollution in the four cities, we analyzed in detail 12 O<sub>3</sub> episodes (three per city; Beijing: 9, 26, 30 July 2005; Shanghai: 7, 8, 22 May 2005; Guangzhou: 18, 23, 24 May 2004; Lanzhou: 5, 11, 12 July 2006). These cases were chosen because elevated O<sub>3</sub> levels were observed and the most comprehensive measurements (i.e., multiple daily VOC samples) were made. (The time series of O<sub>3</sub> and related parameters during these episodes are shown in Figs. S3–S6.) At a given location, the change of O<sub>3</sub> mixing ratios is a combined result of in situ photochemistry, regional transport (both horizontal and vertical) and deposition. The contributions of chemistry and transport can be either positive (i.e., production and import) or negative (i.e., destruction and export). In the present study, we examined the contributions of in situ photochemistry and regional transport to the observed O<sub>3</sub> pollution by using observations coupled with OBM analysis. We first determined the rate of change in O<sub>3</sub> concentrations from the observed O<sub>3</sub> time series ( $R_{\text{meas}}$ ). The in situ net O<sub>3</sub> production ( $R_{\text{chem}}$ ) and deposition rates ( $R_{\text{deps}}$ ) were computed every hour by the OBM as described in Sect. 2.3. Then the difference ( $R_{\text{trans}} =$

$R_{\text{meas}} - R_{\text{chem}} - R_{\text{deps}}$ ) can be considered as the contribution from regional transport (note that the effect of atmospheric mixing was also included in this term).

Figure 4 displays the time series of O<sub>3</sub> and contributions of in situ production, deposition and regional transport for typical O<sub>3</sub> episodes at the four cities (the results were similar for other cases for each city and are not shown). Two interesting phenomena are illustrated. One is the intrusion of residual boundary-layer air contributing to O<sub>3</sub> increase during the early morning period. At all four cities, in particular Lanzhou,  $R_{\text{trans}}$  presented an important contributor to the O<sub>3</sub> increase in the early morning. This should be attributed to mixing with the O<sub>3</sub>-rich air aloft when the nocturnal boundary layer is broken down. The other is the sudden changes of the transport effect corresponding to the variation in surface winds. During the Beijing case (Fig. 4a), for example, the southeasterly winds brought urban plume to the study site, resulting in an O<sub>3</sub> peak at 14:00–15:00 LT; but after that the wind direction shifted to northerly, leading to a sharp O<sub>3</sub> decrease. Similar wind effects were also noticed for the Guangzhou and Lanzhou cases. These results suggest that our method can capture the variations in physical processes and hence is capable of quantifying the contributions of regional transport.

We are particularly interested in the relative roles of in situ photochemistry and transport in the extremely high O<sub>3</sub> levels

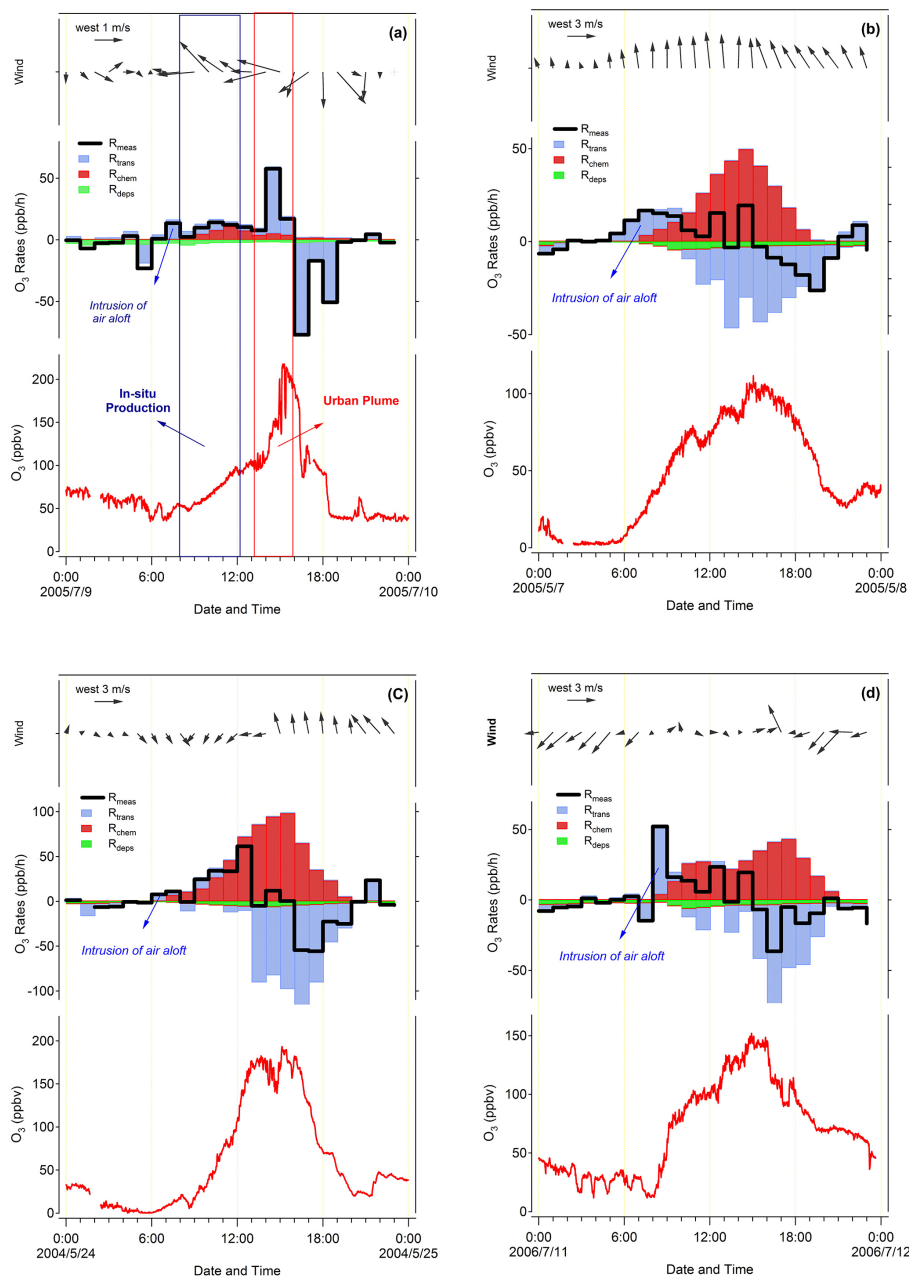


**Figure 4.** O<sub>3</sub> accumulation and contributions from in situ chemistry, regional transport, and deposition during episodes in (a) Beijing (9 July 2005), (b) Shanghai (7 May 2005), (c) Guangzhou (24 May 2004), and (d) Lanzhou (11 July 2006). Note that the blue bars are added to the red ones.

observed at the rural site downwind of Beijing. As shown in Fig. 4a, both in situ production and regional transport contributed to the O<sub>3</sub> accumulation from morning (~40 ppbv at 8:00 LT) to noon (~100 ppbv at 12:00 LT). In the afternoon, however, the O<sub>3</sub> mixing ratios increased sharply from ~100 to ~220 ppbv within less than 2 h (14:00–15:00 LT), during which the in situ O<sub>3</sub> production had been weakened due to the relatively low levels of VOCs and NO<sub>x</sub>. Thus such a sharp O<sub>3</sub> rise was attributed to the transport of urban plumes from

Beijing that had undergone extensive photochemical processing and contained high amounts of produced O<sub>3</sub>. This is a very typical case at CP in summer, and highlights the efficient export of Beijing urban pollution in the afternoon, which can adversely affect the vegetation and crops in downwind areas.

In comparison, the in situ production dominated the O<sub>3</sub> accumulation throughout the daytime at suburban sites downwind of Shanghai, Guangzhou and Lanzhou (see Fig. 4b–d). Very strong O<sub>3</sub> formation was determined during these



episodes (e.g., up to 50, 90 and 40 ppbv h<sup>-1</sup> at Shanghai, Guangzhou and Lanzhou). Regional transport generally made a negative contribution (i.e., export) to the observed O<sub>3</sub> pollution. This indicates that the air masses at these sites were reactive enough to sustain the observed O<sub>3</sub> increase and even had potential to export the produced O<sub>3</sub> to downwind regions.

We then examined the ozone formation regimes in Shanghai, Guangzhou and Lanzhou, where in situ photochemistry dominated the O<sub>3</sub> pollution, by calculating the relative incremental reactivity (RIR) with the OBM. RIR is defined as the ratio of decrease in O<sub>3</sub> production rate to decrease in precursor concentrations, and can be used as a metric for the effect of a given emission reduction on O<sub>3</sub> concentrations (Cardelino and Chameides, 1995). The daytime-average RIRs for major groups of O<sub>3</sub> precursors during the episodes are shown in Fig. 5. Overall, the O<sub>3</sub> formation regimes were consistent among cases for each city but different among cities. In Shanghai and Guangzhou, the in situ O<sub>3</sub> production was highly VOC-sensitive, specifically AHC-controlled (see Fig. 5a). The RIRs for NO<sub>x</sub> were negative. Within the AHC dominated were reactive aromatics and alkenes in Shanghai and aromatics in Guangzhou (see Fig. 5b). This suggests that reducing emissions of aromatics (and also alkenes for Shanghai) would weaken the O<sub>3</sub> formation in both cities, yet cutting NO<sub>x</sub> emissions may aggravate the local O<sub>3</sub> problems.

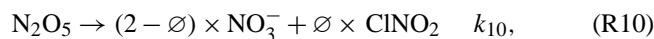
In Lanzhou, the O<sub>3</sub> formation was most sensitive to NO<sub>x</sub> and to a lesser extent to AHC. Within the AHC, alkenes were the most important compounds responsible for the O<sub>3</sub> production. In particular, light olefins such as propene and ethene were the most abundant reactive species, both of which presented approximately half of the AHC reactivity (figure not shown). Such high levels of olefins are attributable to the industrial structure of Lanzhou, which is a well-known petrochemical city in West China with the China National Petroleum Corporation–Lanzhou Petrochemical Company and many small petrochemical plants located in its Xigu district. Light olefins are major components of the petrochemical plant emissions (Ryerson et al., 2003). The results suggest that the most efficient way to alleviate the O<sub>3</sub> pollution in Lanzhou is to cut the NO<sub>x</sub> emissions (from petrochemical and power plants as well as vehicles), while reducing emissions of olefins (from the petrochemical plants) could also result in considerable decrease in O<sub>3</sub> formation.

### 3.3 Impact of heterogeneous processes

In this section, we assess the potential impacts of several poorly understood heterogeneous processes on the ozone production in the four target cities, by incorporating them in the OBM and conducting sensitivity analyses.

#### 3.3.1 ClNO<sub>2</sub> production from N<sub>2</sub>O<sub>5</sub> hydrolysis

The hydrolysis of N<sub>2</sub>O<sub>5</sub> may produce nitryl chloride (ClNO<sub>2</sub>), which is usually accumulated at night and can enhance the next-day's O<sub>3</sub> formation by releasing both NO<sub>2</sub> and chlorine atom (it can oxidize hydrocarbons like OH) via photolysis. The hydrolysis rate is considered to be first order of the N<sub>2</sub>O<sub>5</sub> concentrations (Chang et al., 2011). This process has not been considered by most of the current mechanisms (e.g., MCM), and is here parameterized in our MCM-based model as follows.



where  $\varphi$  is the production yield of ClNO<sub>2</sub>, and  $k_{10}$  is the first order rate constant and estimated by

$$k_{10} = \frac{1}{4} \times v_{\text{N}_2\text{O}_5} \times \gamma_{\text{N}_2\text{O}_5} \times S_{\text{aero}}, \quad (3)$$

where  $v_{\text{N}_2\text{O}_5}$  is the mean molecular speed of N<sub>2</sub>O<sub>5</sub> and can be calculated from the gas kinetic theory (Aldener et al., 2006);  $\gamma_{\text{N}_2\text{O}_5}$  is the reactive uptake coefficient of N<sub>2</sub>O<sub>5</sub> on aerosol surfaces;  $S_{\text{aero}}$  is the aerosol surface area concentration and is calculated based on the measured particle number size distributions. The current uncertainty of this process primarily lies in the uptake coefficient of N<sub>2</sub>O<sub>5</sub> and production yield of ClNO<sub>2</sub>, which are highly variable and dependent on the aerosol composition, humidity and temperature (Chang et al., 2011). The  $\gamma_{\text{N}_2\text{O}_5}$  derived on real atmospheric particles from limited available field observations were in the range of 0–0.04 (Chang et al., 2011, and references therein). In the present study, we adopted a moderate value of  $\gamma_{\text{N}_2\text{O}_5} = 0.03$  with no production of ClNO<sub>2</sub> ( $\varphi = 0$ ) in the base model, and conducted sensitivity analyses by including ClNO<sub>2</sub> production with a moderate yield of 60 %.

Figure 6 illustrates the impacts of ClNO<sub>2</sub> formation from N<sub>2</sub>O<sub>5</sub> hydrolysis on the O<sub>3</sub> production during the selected episodes in the four cities. Overall, the ClNO<sub>2</sub> produced/accumulated at night may enhance considerably the next-day's O<sub>3</sub> formation, and this impact is highly dependent on the abundances of both aerosol surface density (more interface) and nitrogen oxides (more reactants). For instance, including the ClNO<sub>2</sub> formation would result in an average nighttime ClNO<sub>2</sub> peak of 1.3 ppbv at the Shanghai site with high concentrations of both NO<sub>x</sub> and particle surface, which in turn would enhance the daytime-average O<sub>3</sub> production rates by  $\sim 3$  ppbv h<sup>-1</sup> on average (or 14 % in percentage; the enhancement was the most significant in the early morning with the maximum percentage of  $\sim 26$  %, and then decreased over the course of the day). In comparison, this process seems to be less significant ( $< 10$  % for the daytime average) at the other three sites due to their relatively lower levels of NO<sub>x</sub> and/or aerosol surface. It is noteworthy that the OBM cannot take into account the transport of ClNO<sub>2</sub> that has relatively long lifetime at night. ClNO<sub>2</sub> may present

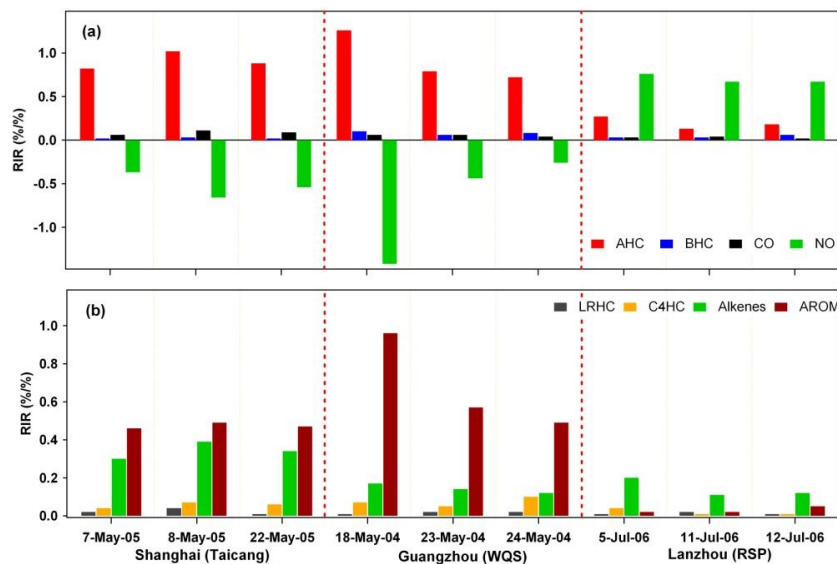


**Figure 5.** The OBM-calculated RIRs for (a) major O<sub>3</sub> precursor groups and (b) the AHC sub-groups during high O<sub>3</sub> events in Shanghai, Guangzhou and Lanzhou.

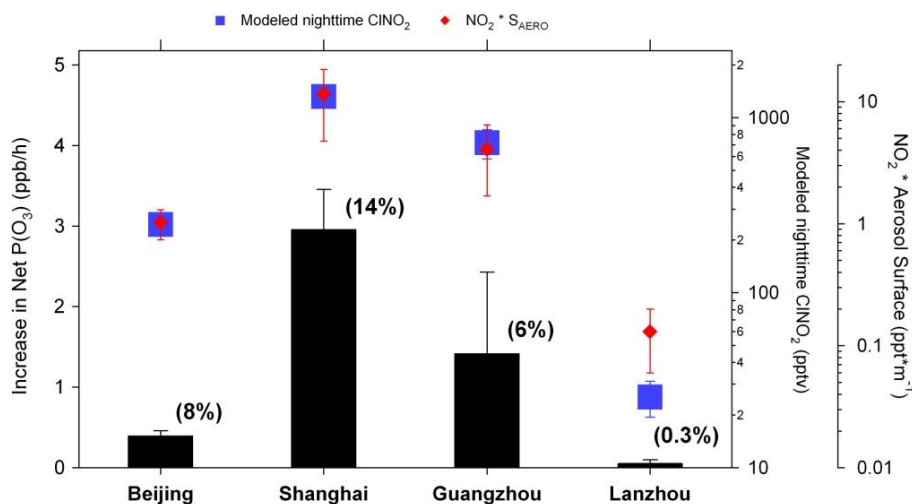


**Figure 6.** Average increase in the daytime-average O<sub>3</sub> production rates by including CINO<sub>2</sub> formation ( $\phi_{\text{CINO}_2} = 0.6$ ) during episodes at four cities. Also shown are the model-simulated nighttime CINO<sub>2</sub> concentrations and the product of NO<sub>2</sub> with aerosol surface. The error bars are standard deviations. The number in parentheses gives the increase in percentage.

a positive altitude profile in the nocturnal boundary layer due to less O<sub>3</sub> titration above the ground. Intrusion of the air aloft in the early morning might contribute considerably to the CINO<sub>2</sub> at surface sites. Therefore, our estimation of the impact of CINO<sub>2</sub> in the present study should be a lower limit. Nonetheless, our results indicate that the nighttime heterogeneous process of N<sub>2</sub>O<sub>5</sub> is a considerable uncertainty in the current understanding of O<sub>3</sub> photochemistry in the high-NO<sub>x</sub> and high-aerosol environments such as Shanghai. Clearly, in situ measurements of N<sub>2</sub>O<sub>5</sub> and CINO<sub>2</sub> are urgently required to better understand this process and to provide more realistic

parameterizations of  $\gamma_{\text{N}_2\text{O}_5}$  and  $\phi_{\text{CINO}_2}$  which can be adopted in air quality models.

### 3.3.2 Uptake of HO<sub>2</sub> by aerosols

The heterogeneous loss of HO<sub>2</sub> on aerosol surface can act as an efficient radical sink at high aerosol loadings and thus attenuate O<sub>3</sub> production (Kanaya et al., 2009). This process is also usually neglected by the current mechanisms, and here was included in our model by adding the following reaction.



The reaction rates were assumed to be first order in the HO<sub>2</sub> concentrations.  $k_{11}$  is the reaction constant that can be calculated by

$$k_{11} = -\left(\frac{r}{D_g + \gamma_{\text{HO}_2}} \times v_{\text{HO}_2}\right)^{-1} S_{\text{aero}}, \quad (4)$$

where  $r$  is the surface-weighted particle radius;  $D_g$  is the gas phase diffusion coefficient and is assumed to be  $0.247 \text{ cm}^2 \text{ s}^{-1}$  (Mozurkewich et al., 1987) (the gas diffusion limitation is accounted for here given the potential larger uptake of HO<sub>2</sub> to aerosol; see below);  $\gamma_{\text{HO}_2}$  is the uptake coefficient of HO<sub>2</sub> on particles;  $v_{\text{HO}_2}$  is the mean molecular speed of HO<sub>2</sub>; and  $S_{\text{aero}}$  is the aerosol surface density. Similar to N<sub>2</sub>O<sub>5</sub> hydrolysis, the uptake coefficient ( $\gamma_{\text{HO}_2}$ ) is a parameter with large uncertainty and is related to the aerosol composition, temperature and RH (Thornton et al., 2008). The laboratory studies determined the  $\gamma_{\text{HO}_2}$  in the range of 0.01–0.2 for different types of non-metal aerosols at room temperatures, with much higher values (>0.2) measured on the Cu-doped aqueous surfaces (Mao et al., 2010, and references therein). Taketani et al. (2012) recently reported relatively large  $\gamma_{\text{HO}_2}$  values for ambient aerosols at Mt. Tai (0.13–0.34) and Mt. Mang (0.09–0.40) in China. Here we adopted a value of  $\gamma_{\text{HO}_2} = 0.02$  in the base model, and changed it to an upper limit (0.4) for sensitivity model runs.

Figure 7 elucidates the effects of heterogeneous HO<sub>2</sub> loss on the modeled HO<sub>2</sub> concentrations and O<sub>3</sub> production rates during episodes in the four cities. Varying impacts of this process in different cities are clearly illustrated. These impacts mainly depend on the abundances of aerosol surface, and are also related to the levels of nitrogen oxides (i.e., at high-NO<sub>x</sub> conditions, the HO<sub>2</sub> loss is dominated by its reactions with NO<sub>x</sub> and its heterogeneous loss is less important) as well as the O<sub>3</sub> formation regimes (i.e., the same HO<sub>2</sub> reduction would lead to less reduction in O<sub>3</sub> formation at NO<sub>x</sub>-limited regime than at the VOCs-limited regime). At the Shanghai, Guangzhou and Lanzhou sites with relatively higher levels of NO<sub>x</sub> or lower loadings of aerosols, adopting a higher uptake coefficient ( $\gamma_{\text{HO}_2} = 0.4$ ) would only lead to little to moderate reductions in the HO<sub>2</sub> concentrations (<21 %) and O<sub>3</sub> production rates (<10 %). At the Beijing site, however, a faster uptake would reduce significantly the HO<sub>2</sub> levels by about 50 % due to its very high loadings of aerosol surface ( $\sim 1600 \mu\text{m}^2 \text{ cm}^{-3}$ ). Such HO<sub>2</sub> reduction would in turn result in an average decrease of  $\sim 15$  % in the daytime-average O<sub>3</sub> production rates (note that a relatively smaller reduction in O<sub>3</sub> production should be attributed to the more NO<sub>x</sub>-sensitive O<sub>3</sub> production regime at our rural site). This indicates that the uptake of HO<sub>2</sub> presents another large source of uncertainty in current studies of O<sub>3</sub> photochemistry in the high-aerosol environments like Beijing, and more observational studies are required to quantify the  $\gamma_{\text{HO}_2}$  on the real particles.

### 3.3.3 Surface reactions of NO<sub>2</sub> forming HONO

HONO is a key reservoir of the hydroxyl radical (OH) and hence plays a crucial role in atmospheric chemistry. Recent studies have indicated possible existence of “missing” source(s) for daytime HONO, which cannot be reproduced by current models only considering the homogeneous source from the OH + NO reaction (e.g., Su et al., 2008, 2011). It has been suggested that the photo-enhanced heterogeneous reactions of NO<sub>2</sub> on various surfaces should be an important source of HONO (Su et al., 2008; Li et al., 2010). In the present study, HONO was not measured but simulated within the model. In addition to the homogeneous source, heterogeneous sources from reactions of NO<sub>2</sub> on the ground and aerosol surfaces were also taken into account in the base model by adopting the parameterizations used by Li et al. (2010). The reaction rates were assumed to be first order of the NO<sub>2</sub> concentrations (Aumont et al., 2003), and the processes were simplified as follows.



$k_g$  and  $k_a$  are the first order rate constants for the ground and aerosol surface reactions, and can be estimated as

$$k_g = \frac{1}{8} \times v_{\text{NO}_2} \times \gamma_g \times \left(\frac{S}{V}\right) \quad (5)$$

$$k_a = \frac{1}{4} \times v_{\text{NO}_2} \times \gamma_a \times S_{\text{aero}}, \quad (6)$$

where  $v_{\text{NO}_2}$  is the mean molecular speed of NO<sub>2</sub>;  $\gamma_g$  and  $\gamma_a$  are the uptake coefficients of NO<sub>2</sub> on the ground and aerosol surfaces;  $S/V$  is the effective surface density of the ground, and  $S_{\text{aero}}$  is the aerosol surface area concentration. Considering the photo-enhanced production of HONO from the surface reactions (George, 2005; Monge et al., 2010), higher values of  $\gamma_g$  and  $\gamma_a$  were used during the daytime than at night. For  $\gamma_g$ , we used a value of  $\gamma_g = 1 \times 10^{-6}$  at nighttime, and increased it to  $2 \times 10^{-5}$  during the daytime with solar radiation smaller than  $400 \text{ W m}^{-2}$ . With more intense solar radiation, a higher  $\gamma_g$  value of  $2 \times 10^{-5} \times (\text{solar radiation}/400)$  was used (Li et al., 2010). As to  $\gamma_a$ , we used a value of  $\gamma_a = 1 \times 10^{-6}$  at nighttime and increased it to  $5 \times 10^{-6}$  during the day, according to Li et al. (2010). An effective surface area of  $1.7 \text{ m}^2$  per geometric ground surface was used to calculate the  $S/V$  (Vogel et al., 2003).

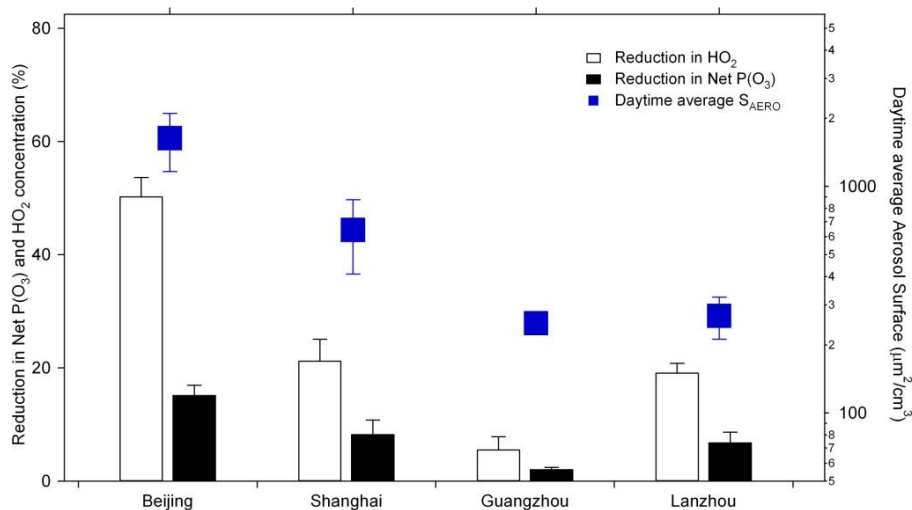


**Figure 7.** Average reductions in the daytime-average HO<sub>2</sub> concentrations and O<sub>3</sub> production rates by adjusting  $\gamma_{\text{HO}_2}$  from 0.02 to 0.4 during episodes at four cities. Also shown are the observed aerosol surface area concentrations (note that the data in Guangzhou were inferred from the measurements at a nearby station in Hong Kong). The error bars are standard deviations.

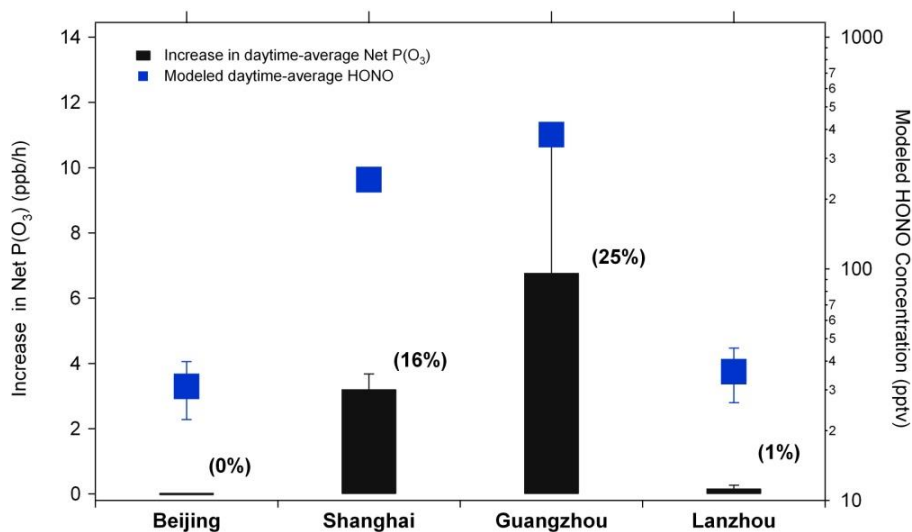


**Figure 8.** Average increase in the daytime-average O<sub>3</sub> production rate by including HONO formation from heterogeneous NO<sub>2</sub> reactions during episodes at four cities. Also shown are the modeled daytime-average HONO concentrations. The error bars are standard deviations. The number in parentheses gives the increase in percentage.

The heterogeneous HONO formation may enhance O<sub>3</sub> production by releasing OH via HONO photolysis. We conducted sensitivity model runs by turning off the heterogeneous HONO sources, which is the case of most current atmospheric models. The results are shown in Fig. 8. We can see that including these processes would enhance the daytime-average O<sub>3</sub> production rates by  $\sim 6.8$  and  $\sim 3.2$  ppb h<sup>-1</sup> on average ( $\sim 25$  and  $\sim 16$ %) in Shanghai and Guangzhou respectively, but lead to little change for the Beijing and Lanzhou sites ( $< 1$ %). This corresponds well to the distributions of nitrogen oxides observed at the four sites (see

Fig. 2). And aerosol surface loading seems not a key factor here, which is in line with the fact that the heterogeneous HONO formation on the ground generally dominates than those on the aerosol at the ground level (Su et al., 2008). These results suggest that the heterogeneous processes of NO<sub>2</sub> may play an important role in atmospheric photochemistry in the high-NO<sub>x</sub> environments such as Shanghai and Guangzhou, and need to be included in the air quality models.

In situ measurements of HONO, which were not available in China until recent years, have shown surprisingly elevated

concentrations of HONO (up to the ppb level) throughout the daytime in the PRD region (e.g., Su et al., 2008). Such high levels of daytime HONO cannot be explained by only including the above heterogeneous reactions of  $\text{NO}_2$ , and some additional sources have been proposed (e.g., Su et al., 2011). It is not known if this phenomenon was also the case at our study sites, however identification of additional HONO source(s) is beyond the scope of the present study. The analyses presented here clearly indicate that the surface reactions of  $\text{NO}_2$  at least present an important HONO source and can enhance  $\text{O}_3$  production. Undoubtedly, in situ measurements of HONO are critical for better understanding the atmospheric photochemistry including  $\text{O}_3$  formation, and further efforts are needed to determine the “missing” source(s).

#### 4 Summary

Measurements of  $\text{O}_3$  and  $\text{O}_3$  precursors were made at a rural site downwind of Beijing and suburban sites at Shanghai, Guangzhou and Lanzhou. The data were analyzed to elucidate the  $\text{O}_3$  precursor distributions, roles of transport and in situ production, and impacts of heterogeneous processes. The major findings are summarized as follows.

1. The four cities suffered from severe  $\text{O}_3$  pollution and showed different precursor distributions. The  $\text{NO}_y$  levels in Shanghai and Guangzhou were higher than that in Lanzhou, while an opposite pattern was found for the VOC reactivity. The dominant anthropogenic hydrocarbons were alkenes in Lanzhou, aromatics in Guangzhou, and both alkenes and aromatics in Beijing and Shanghai.
2. Transport of “aged” urban plumes resulted in the extremely high  $\text{O}_3$  levels (up to 286 ppbv) at the rural site downwind of Beijing, while intense in situ photochemical production dominated at the suburban sites of Shanghai, Guangzhou and Lanzhou. The  $\text{O}_3$  production was VOCs-limited in Shanghai and Guangzhou and  $\text{NO}_x$ -limited in Lanzhou. The key VOC species were aromatics and alkenes in Shanghai and aromatics in Guangzhou.
3. The potential impacts of several poorly understood heterogeneous processes on  $\text{O}_3$  production were assessed. The  $\text{N}_2\text{O}_5$  hydrolysis was more significant at the Shanghai site due to its high levels of both aerosol and  $\text{NO}_x$ . The  $\text{HO}_2$  loss on aerosols was more relevant for Beijing because of its very high aerosol loadings. The HONO formation from surface reactions of  $\text{NO}_2$  was more important for the Guangzhou and Shanghai sites mainly owing to their high  $\text{NO}_x$  levels. And the  $\text{O}_3$  production at the Lanzhou site seemed to be less sensitive to all of these processes due to its relatively low concentrations

of aerosol and  $\text{NO}_x$ . These findings indicate the varying impacts of heterogeneous processes on the  $\text{O}_3$  photochemistry in different regions of China, and suggest further necessity to better understand these processes.

4. In summary, the results of this study have provided insights into  $\text{O}_3$  pollution, local chemistry versus outside impact, and potential impacts of heterogeneous chemistry in major urban areas of China. The high-quality data taken in the mid-2000s will be particularly valuable for assessing the atmospheric impact of rapid urbanization/industrialization process in China.

**The Supplement related to this article is available online at doi:10.5194/acp-14-13175-2014-supplement.**

*Acknowledgements.* The authors are grateful to Steven Poon, Waisheng Wu and Jiamin Zhang for their contributions to the field work, and to Tijian Wang and Jie Tang for their help in selecting the study sites. We would like to thank the Master Chemical Mechanism group in University of Leeds for providing the mechanism. We also appreciate two anonymous reviewers who raised helpful comments to improve our manuscript. The field measurements were funded by the Research Grants Council of Hong Kong (HKRGC; PolyU5144/04E), and the data analysis was supported by the Hong Kong Polytechnic University (1-BB94 and 1-ZV9N) and the HKRGC (PolyU5015/12P).

Edited by: X. Tie

#### References

- Aldener, M., Brown, S., Stark, H., Williams, E., Lerner, B., Kuster, W., Goldan, P., Quinn, P., Bates, T., and Fehsenfeld, F.: Reactivity and loss mechanisms of  $\text{NO}_3$  and  $\text{N}_2\text{O}_5$  in a polluted marine environment: Results from in situ measurements during New England Air Quality Study 2002, *J. Geophys. Res.*, 111, D23S73, doi:10.1029/2006JD007252, 2006.
- Aumont, B., Chervier, F., and Laval, S.: Contribution of HONO sources to the  $\text{NO}_x/\text{HO}_x/\text{O}_3$  chemistry in the polluted boundary layer, *Atmos. Environ.*, 37, 487–498, 2003.
- Berlin, S. R., Langford, A. O., Estes, M., Dong, M., and Parrish, D. D.: Magnitude, decadal changes, and impact of regional background ozone transported into the greater Houston, Texas Area, *Environ. Sci. Tech.*, 47, 13985–13992, 2013.
- Brown, S. S., Ryerson, T. B., Wollny, A. G., Brock, C. A., Peltier, R., Sullivan, A. P., Weber, R. J., Dube, W. P., Trainer, M., Meagher, J. F., Fehsenfeld, F. C., and Ravishankara, A. R.: Variability in nocturnal nitrogen oxide processing and its role in regional air quality, *Science*, 311, 67–70, 2006.
- Cardelino, C. A. and Chameides, W. L.: An Observation-Based Model for Analyzing Ozone Precursor Relationships in the Urban Atmosphere, *J. Air Waste Manage.*, 45, 161–180, 1995.

- Chang, W. L., Bhave, P. V., Brown, S. S., Riemer, N., Stutz, J., and Dabdub, D.: Heterogeneous Atmospheric Chemistry, Ambient Measurements, and Model Calculations of  $\text{N}_2\text{O}_5$ : A Review, *Aerosol Sci Tech.*, 45, 665–695, 2011.
- Chou, C. C.-K., Tsai, C.-Y., Chang, C.-C., Lin, P.-H., Liu, S. C., and Zhu, T.: Photochemical production of ozone in Beijing during the 2008 Olympic Games, *Atmos. Chem. Phys.*, 11, 9825–9837, doi:10.5194/acp-11-9825-2011, 2011.
- Ding, A. J., Wang, T., Thouret, V., Cammas, J.-P., and Nédélec, P.: Tropospheric ozone climatology over Beijing: analysis of aircraft data from the MOZAIC program, *Atmos. Chem. Phys.*, 8, 1–13, doi:10.5194/acp-8-1-2008, 2008.
- Ding, A. J., Fu, C. B., Yang, X. Q., Sun, J. N., Zheng, L. F., Xie, Y. N., Herrmann, E., Nie, W., Petäjä, T., Kerminen, V.-M., and Kulmala, M.: Ozone and fine particle in the western Yangtze River Delta: an overview of 1 yr data at the SORPES station, *Atmos. Chem. Phys.*, 13, 5813–5830, doi:10.5194/acp-13-5813-2013, 2013.
- Frost, G. J., Trainer, M., Allwine, G., Buhr, M. P., Calvert, J. G., Cantrell, C. A., Fehsenfeld, F. C., Goldan, P. D., Herwehe, J., Hubler, G., Kuster, W. C., Martin, R., McMillen, R. T., Montzka, S. A., Norton, R. B., Parrish, D. D., Ridley, B. A., Shetter, R. E., Walega, J. G., Watkins, B. A., Westberg, H. H., and Williams, E. J.: Photochemical ozone production in the rural southeastern United States during the 1990 Rural Oxidants in the Southern Environment (ROSE) program, *J. Geophys. Res.-Atmos.*, 103, 22491–22508, 1998.
- Gao, J., Wang, T., Zhou, X. H., Wu, W. S., and Wang, W. X.: Measurement of aerosol number size distributions in the Yangtze River delta in China: Formation and growth of particles under polluted conditions, *Atmos. Environ.*, 43, 829–836, 2009.
- George, C., Strekowski, R., Kleffmann, J., Stemmler, K., and Ammann, M.: Photoenhanced uptake of gaseous  $\text{NO}_2$  on solid organic compounds: a photochemical source of  $\text{HONO}$ ?, *Faraday Discuss.*, 130, 195–210, 2005.
- Jacob, D. J.: Introduction to Atmospheric Chemistry, Princeton University Press, Princeton, New Jersey, 1999.
- Jenkin, M. E., Saunders, S. M., Wagner, V., and Pilling, M. J.: Protocol for the development of the Master Chemical Mechanism, MCM v3 (Part B): tropospheric degradation of aromatic volatile organic compounds, *Atmos. Chem. Phys.*, 3, 181–193, doi:10.5194/acp-3-181-2003, 2003.
- Kanaya, Y., Pochanart, P., Liu, Y., Li, J., Tanimoto, H., Kato, S., Suthawaree, J., Inomata, S., Taketani, F., Okuzawa, K., Kawamura, K., Akimoto, H., and Wang, Z. F.: Rates and regimes of photochemical ozone production over Central East China in June 2006: a box model analysis using comprehensive measurements of ozone precursors, *Atmos. Chem. Phys.*, 9, 7711–7723, doi:10.5194/acp-9-7711-2009, 2009.
- Li, G., Lei, W., Zavala, M., Volkamer, R., Dusanter, S., Stevens, P., and Molina, L. T.: Impacts of HONO sources on the photochemistry in Mexico City during the MCMA-2006/MILAGO Campaign, *Atmos. Chem. Phys.*, 10, 6551–6567, doi:10.5194/acp-10-6551-2010, 2010.
- Liu, Z., Wang, Y., Gu, D., Zhao, C., Huey, L. G., Stickel, R., Liao, J., Shao, M., Zhu, T., Zeng, L., Amoroso, A., Costabile, F., Chang, C.-C., and Liu, S.-C.: Summertime photochemistry during CAREBeijing-2007:  $\text{RO}_x$  budgets and  $\text{O}_3$  formation, *Atmos. Chem. Phys.*, 12, 7737–7752, doi:10.5194/acp-12-7737-2012, 2012.
- Mao, J., Jacob, D. J., Evans, M. J., Olson, J. R., Ren, X., Brune, W. H., Clair, J. M. St., Crouse, J. D., Spencer, K. M., Beaver, M. R., Wennberg, P. O., Cubison, M. J., Jimenez, J. L., Fried, A., Weibring, P., Walega, J. G., Hall, S. R., Weinheimer, A. J., Cohen, R. C., Chen, G., Crawford, J. H., McNaughton, C., Clarke, A. D., Jaeglé, L., Fisher, J. A., Yantosca, R. M., Le Sager, P., and Carouge, C.: Chemistry of hydrogen oxide radicals ( $\text{HO}_x$ ) in the Arctic troposphere in spring, *Atmos. Chem. Phys.*, 10, 5823–5838, doi:10.5194/acp-10-5823-2010, 2010.
- Monge, M. E., D'Anna, B., Mazri, L., Giroir-Fendler, A., Ammann, M., Donaldson, D. J., and George, C.: Light changes the atmospheric reactivity of soot, *Proc. Natl. Acad. Sci.*, 107, 6605–6609, 2010.
- Molina, M. J. and Molina, L. T.: Megacities and atmospheric pollution, *J. Air Waste Manage.*, 54, 644–680, 2004.
- Mozurkewich, M., McMurry, P. H., Gupta, A., and Calvert, J. G.: Mass accommodation coefficient of  $\text{HO}_2$  on aqueous particles, *J. Geophys. Res.*, 92, 4163–4170, 1987.
- Ohara, T., Akimoto, H., Kurokawa, J., Horii, N., Yamaji, K., Yan, X., and Hayasaka, T.: An Asian emission inventory of anthropogenic emission sources for the period 1980–2020, *Atmos. Chem. Phys.*, 7, 4419–4444, doi:10.5194/acp-7-4419-2007, 2007.
- Parrish, D. D. and Zhu, T.: Clean Air for Megacities, , 326, 674–675, 2009.
- Pathak, R. K., Wu, W. S., and Wang, T.: Summertime  $\text{PM}_{2.5}$  ionic species in four major cities of China: nitrate formation in an ammonia-deficient atmosphere, *Atmos. Chem. Phys.*, 9, 1711–1722, doi:10.5194/acp-9-1711-2009, 2009.
- Ran, L., Zhao, C. S., Geng, F. H., Tie, X. X., Tang, X., Peng, L., Zhou, G. Q., Yu, Q., Xu, J. M., and Guenther, A.: Ozone photochemical production in urban Shanghai, China: Analysis based on ground level observations, *J. Geophys. Res.-Atmos.*, 114, D15301, doi:10.1029/2008JD010752, 2009.
- Ryerson, T. B., Trainer, M., Angevine, W. M., Brock, C. A., Dissly, R. W., Fehsenfeld, F. C., Frost, G. J., Goldan, P. D., Holloway, J. S., Hubler, G., Jakoubek, R. O., Kuster, W. C., Neuman, J. A., Nicks Jr., D. K., Parrish, D. D., Roberts, J. M., and Sueper, D. T.: Effect of petrochemical industrial emissions of reactive alkenes and  $\text{NO}_x$  on tropospheric ozone formation in Houston, Texas, *J. Geophys. Res.-Atmos.*, 108, 4249, doi:10.1029/2002JD003070, 2003.
- Saunders, S. M., Jenkin, M. E., Derwent, R. G., and Pilling, M. J.: Protocol for the development of the Master Chemical Mechanism, MCM v3 (Part A): tropospheric degradation of non-aromatic volatile organic compounds, *Atmos. Chem. Phys.*, 3, 161–180, doi:10.5194/acp-3-161-2003, 2003.
- Stockwell, W. R., Lawson, C. V., Saunders, E., and Goliff, W. S.: A review of tropospheric atmospheric chemistry and gas-phase chemical mechanisms for air quality modeling, *Atmosphere*, 3, 1–32, 2012.
- Su, H., Cheng, Y. F., Shao, M., Gao, D. F., Yu, Z. Y., Zeng, L. M., Slanina, J., Zhang, Y. H., and Wiedensohler, A.: Nitrous acid ( $\text{HONO}$ ) and its daytime sources at a rural site during the 2004 PRIDE-PRD experiment in China, *J. Geophys. Res.-Atmos.*, 113, D14312, doi:10.1029/2007JD009060, 2008.



- Su, H., Cheng, Y. F., Oswald, R., Behrendt, T., Trebs, I., Meixner, F. X., Andreae, M. O., Cheng, P., Zhang, Y., and Pöschl, U.: Soil Nitrite as a Source of Atmospheric HONO and OH Radicals, *Science*, 333, 1616–1618, 2011.
- Taketani, F., Kanaya, Y., Pochanart, P., Liu, Y., Li, J., Okuzawa, K., Kawamura, K., Wang, Z., and Akimoto, H.: Measurement of overall uptake coefficients for HO<sub>2</sub> radicals by aerosol particles sampled from ambient air at Mts. Tai and Mang (China), *Atmos. Chem. Phys.*, 12, 11907–11916, doi:10.5194/acp-12-11907-2012, 2012.
- Thornton, J. A., Jaegle, L., and McNeill, V. F.: Assessing known pathways for HO<sub>2</sub> loss in aqueous atmospheric aerosols: Regional and global impacts on tropospheric oxidants, *J. Geophys. Res.-Atmos.*, 113, D05303, doi:10.1029/2007JD009236, 2008.
- Tie, X., Geng, F., Guenther, A., Cao, J., Greenberg, J., Zhang, R., Apel, E., Li, G., Weinheimer, A., Chen, J., and Cai, C.: Megacity impacts on regional ozone formation: observations and WRF-Chem modeling for the MIRAGE-Shanghai field campaign, *Atmos. Chem. Phys.*, 13, 5655–5669, doi:10.5194/acp-13-5655-2013, 2013.
- Vogel, B., Vogel, H., Kleffmann, J., and Kurtenbach, R.: Measured and simulated vertical profiles of nitrous acid – Part II. Model simulations and indications for a photolytic source, *Atmos. Environ.*, 37, 2957–2966, 2003.
- Wang, T., Ding, A. J., Gao, J., and Wu, W. S.: Strong ozone production in urban plumes from Beijing, China, *Geophys. Res. Lett.*, 33, L21806, doi:10.1029/2006GL027689, 2006.
- Wang, T., Wei, X. L., Ding, A. J., Poon, C. N., Lam, K. S., Li, Y. S., Chan, L. Y., and Anson, M.: Increasing surface ozone concentrations in the background atmosphere of Southern China, 1994–2007, *Atmos. Chem. Phys.*, 9, 6217–6227, doi:10.5194/acp-9-6217-2009, 2009.
- Wang, T., Nie, W., Gao, J., Xue, L. K., Gao, X. M., Wang, X. F., Qiu, J., Poon, C. N., Meinardi, S., Blake, D., Wang, S. L., Ding, A. J., Chai, F. H., Zhang, Q. Z., and Wang, W. X.: Air quality during the 2008 Beijing Olympics: secondary pollutants and regional impact, *Atmos. Chem. Phys.*, 10, 7603–7615, doi:10.5194/acp-10-7603-2010, 2010a.
- Wang, X., Zhang, Y., Hu, Y., Zhou, W., Lu, K., Zhong, L., Zeng, L., Shao, M., Hu, M., and Russell, A. G.: Process analysis and sensitivity study of regional ozone formation over the Pearl River Delta, China, during the PRIDE-PRD2004 campaign using the Community Multiscale Air Quality modeling system, *Atmos. Chem. Phys.*, 10, 4423–4437, doi:10.5194/acp-10-4423-2010, 2010b.
- Xu, X., Lin, W., Wang, T., Yan, P., Tang, J., Meng, Z., and Wang, Y.: Long-term trend of surface ozone at a regional background station in eastern China 1991–2006: enhanced variability, *Atmos. Chem. Phys.*, 8, 2595–2607, doi:10.5194/acp-8-2595-2008, 2008.
- Xue, L. K., Wang, T., Zhang, J. M., Zhang, X. C., Deliger, Poon, C. N., Ding, A. J., Zhou, X. H., Wu, W. S., Tang, J., Zhang, Q. Z., and Wang, W. X.: Source of surface ozone and reactive nitrogen speciation at Mount Waliguan in western China: New insights from the 2006 summer study, *J. Geophys. Res.-Atmos.*, 116, D07306, doi:10.1029/2010JD014735, 2011.
- Xue, L. K., Wang, T., Guo, H., Blake, D. R., Tang, J., Zhang, X. C., Saunders, S. M., and Wang, W. X.: Sources and photochemistry of volatile organic compounds in the remote atmosphere of western China: results from the Mt. Waliguan Observatory, *Atmos. Chem. Phys.*, 13, 8551–8567, doi:10.5194/acp-13-8551-2013, 2013.
- Xue, L. K., Wang, T., Louie, P. K. K., Luk, C. W. Y., Blake, D. R., and Xu, Z.: Increasing external effects negate local efforts to control ozone air pollution: a case study of Hong Kong and implications for other Chinese cities, *Environ. Sci. Tech.*, 48, 10769–10775, 2014a.
- Xue, L. K., Wang, T., Wang, X. F., Blake, D. R., Gao, J., Nie, W., Gao, R., Gao, X. M., Xu, Z., Ding, A. J., Huang, Y., Lee, S. C., Chen, Y. Z., Wang, S. L., Chai, F. H., Zhang, Q. Z., and Wang, W. X.: On the use of an explicit chemical mechanism to dissect peroxy acetyl nitrate formation, *Environ. Pollution*, 195, 39–47, 2014b.
- Zhang, J., Wang, T., Chameides, W. L., Cardelino, C., Kwok, J., Blake, D. R., Ding, A., and So, K. L.: Ozone production and hydrocarbon reactivity in Hong Kong, Southern China, *Atmos. Chem. Phys.*, 7, 557–573, doi:10.5194/acp-7-557-2007, 2007.
- Zhang, J. M., Wang, T., Ding, A. J., Zhou, X. H., Xue, L. K., Poon, C. N., Wu, W. S., Gao, J., Zuo, H. C., Chen, J. M., Zhang, X. C., and Fan, S. J.: Continuous measurement of peroxyacetyl nitrate (PAN) in suburban and remote areas of western China, *Atmos. Environ.*, 43, 228–237, 2009.
- Zhang, L., Chen, C. H., Li, S. X., and Zhang, F.: Air pollution and potential control schemes in Lanzhou, *Res. Environ. Sci.*, 13, 18–21, 2000.
- Zhang, L., Brook, J. R., and Vet, R.: A revised parameterization for gaseous dry deposition in air-quality models, *Atmos. Chem. Phys.*, 3, 2067–2082, doi:10.5194/acp-3-2067-2003, 2003.
- Zhang, Q., Streets, D. G., Carmichael, G. R., He, K. B., Huo, H., Kannari, A., Klimont, Z., Park, I. S., Reddy, S., Fu, J. S., Chen, D., Duan, L., Lei, Y., Wang, L. T., and Yao, Z. L.: Asian emissions in 2006 for the NASA INTEX-B mission, *Atmos. Chem. Phys.*, 9, 5131–5153, doi:10.5194/acp-9-5131-2009, 2009.
- Zhang, Q., Yuan, B., Shao, M., Wang, X., Lu, S., Lu, K., Wang, M., Chen, L., Chang, C.-C., and Liu, S. C.: Variations of ground-level O<sub>3</sub> and its precursors in Beijing in summertime between 2005 and 2011, *Atmos. Chem. Phys.*, 14, 6089–6101, doi:10.5194/acp-14-6089-2014, 2014.
- Zhang, Y. H., Su, H., Zhong, L. J., Cheng, Y. F., Zeng, L. M., Wang, X. S., Xiang, Y. R., Wang, J. L., Gao, D. F., Shao, M., Fan, S. J., and Liu, S. C.: Regional ozone pollution and observation-based approach for analyzing ozone-precursor relationship during the PRIDE-PRD2004 campaign, *Atmos. Environ.*, 42, 6203–6218, 2008.